Two Conserved Residues Are Important for Inducing Highly Ordered Membrane Domains by the Transmembrane Domain of Influenza Hemagglutinin

Mingtao Ge and Jack H. Freed*
National Biomedical Center for Advanced ESR Technology, Department of Chemistry and Chemical Biology, Cornell University, Ithaca, New York

ABSTRACT The interaction with lipids of a synthetic peptide corresponding to the transmembrane domain of influenza hemagglutinin was investigated by means of electron spin resonance. A detailed analysis of the electron spin resonance spectra from spin-labeled phospholipids revealed that the major effect of the peptide on the dynamic membrane structure is to induce highly ordered membrane domains that are associated with electrostatic interactions between the peptide and negatively charged lipids. Two highly conserved residues in the peptide were identified as being important for the membrane ordering effect. Aggregation of large unilamellar vesicles induced by the peptide was also found to be correlated with the membrane ordering effect of the peptide, indicating that an increase in membrane ordering, i.e., membrane dehydration, is important for vesicle aggregation. The possibility that hydrophobic interaction between the highly ordered membrane domains plays a role in vesicle aggregation and viral fusion is discussed.

INTRODUCTION

Fusion proteins (1) catalyze viral membrane fusion (2,3) through interactions of their multiple components, such as the fusion peptide (FP), haptad repeats, and the transmembrane (TM) domain, with the cellular and viral membranes (4).

It has been shown that TM domains in glycoproteins of *Autographa californica* multicapsid nucleopolyhedrovirus (5,6) and severe acute respiratory syndrome coronavirus (7) play important roles in the budding and entry of these viruses. Replacing the natural TM domain of hemagglutinin (HA) from influenza virus with a glycophosphoinositol-linked lipid anchor results in hemifusion, not complete fusion (8). The TM of HA was also found to be involved in association of HA in lipid raft microdomains, which provide a sufficient concentration of HA in budding virus to mediate virus-cell fusion (9). However, it is not clear how the TM domains function during these viral activities.

It has long been appreciated that membrane dehydration is important for membrane fusion (10–14). A study of interactions of a synthetic peptide representing the TM domain of HA with model membranes revealed that the peptide, which forms a coiled-coil in the membrane, increased the ordering of the lipids (15). Furthermore, it was recently reported that this TM peptide dehydrates the membranes (16). We previously showed that the FP of HA increases the ordering of the bilayer surface at acidic pH, implying that it also dehydrates the membranes (10). Consider the current hairpin model for viral membrane fusion (1–3), which holds that upon acidification, HA undergoes conformational changes, forming a hairpin structure. Its FP inserts into the cell membrane, and its TM domain is fixed at the viral membrane, thus bringing two membranes into close proximity. Consequently, the cell membrane is dehydrated by the FP, and the viral membrane is dehydrated by the TM, which would create a local hydrophobic zone right at the fusion site around the HA hairpins. We are particularly interested in what effects this local membrane dehydration might have on viral fusion.

In this study, we carefully analyzed electron spin resonance (ESR) spectra from spin-labeled lipids to examine changes in the membrane structure induced by the TM from HA, and we also performed turbidity measurements to investigate the relation between these changes and vesicle aggregation. We found that the membrane ordering effect of the TM manifests itself by inducing highly ordered (and thus dehydrated) membrane domains. We suggest that the hydrophobic interaction between these membrane domains may be important for vesicle aggregation and the initial contact between cellular and viral membranes during viral fusion.

MATERIALS AND METHODS

Materials

Lipids (dimyristoylphosphatidylcholine (DMPC), dimyristoylphosphatidylglycerol (DMPG), and liver total lipid extract from bovine (LLE)), two chain spin labels (5PC and 14PC), and a headgroup spin label (dipalmitoylphospatidyl-tempo-choine (DPPTC)) were purchased from Avanti (Alabaster, AL). Cholesterol (Chol) was obtained from Sigma (St. Louis, MO). The peptide of the wild-type (wt) TM domain of HA from influenza (strain X31), TM-wt, and its two mutations (TM-mut1 and TM-mut2) were synthesized by SynBioSci (Livermore, CA) and Biomatik (Silverland, DE) as follows:

TM-wt GYKDWILWISFAISCFLLCVVLLGFIMWACQRG
TM-mut1 GYEDWILWISFAISCFLLCVVLLGFIMWACQRG
TM-mut2 GYKDWIAWISFAISCFLLCVVLLGFIMWACQRG

Submitted August 3, 2010, and accepted for publication November 8, 2010.

*Correspondence: jhf3@cornell.edu

Editor: David D. Thomas.

0006-3495/11/01/0090/8 $2.00

doi: 10.1016/j.bpj.2010.11.014

Preparation of spin-labeled multilamellar vesicles of DMPC/DMPG/Chol and LLE, incorporated with TM (TM-wt, TM-mut1, TM-mut2) and large unilamellar vesicles of LLE

Measured stock solutions of DMPC (in chloroform), DMPG (in chloroform, methanol, and water), Chol (in chloroform), the spin label (in chloroform), and TM (in hexafluoro-isopropanol (HFIP)) were mixed. The concentration of spin label was 0.5 mol % of the lipids. The solvent was evaporated by N_2 flow, and the sample was evacuated with a mechanical pump overnight to remove traces of the solvent. Each sample (1 mg) was hydrated in 30 μL of pH 7 buffer (Tris 10 mM, NaCl 150 mM, EDTA 0.1 mM) at room temperature overnight. Spin-labeled multilamellar vesicles (MLVs) of LLE containing TM were prepared in a similar way. The vesicles were spun in a desktop centrifuge to produce a pellet, which was transferred to a quartz capillary tube for ESR measurement shortly thereafter.

Preparation of large unilamellar vesicles (LUV) of LLE: 1 mg dried LLE (prepared in the same way as above, but without spin label) was hydrated with 2 mL pH 7 buffer (10 mM Tris, 150 mM NaCl, 0.1 mM EDTA) for 1 h. The vesicle solution was vortexed for 1 min and extruded through a 0.1 μm film in an extruder (Lipex Biomembranes, Vancouver, British Columbia, Canada) five times.

ESR measurements and nonlinear least-squares fits of ESR spectra

ESR spectra were recorded at a frequency of 9.55 GHz with an EMX ESR spectrometer (Bruker Instruments) equipped with a Varian temperature control unit with an absolute temperature accuracy of $\pm 0.3^{\circ}$C. The spectra were analyzed with the use of a nonlinear least-squares (NLLS) fitting program (17) based on the stochastic Liouville equation (18,19). The spectral analysis generated two sets of parameters that characterize the rotational diffusion of the nitroxide radical in spin labels. The first set consists of $R_\perp$ and $R_\parallel$, which are respectively the rates of rotation of the nitroxide radical around a molecular axis perpendicular and parallel to the preferential orienting axis of the acyl chain. The second set consists of the ordering tensor parameters, $\mathbf{S}_0$ and $\mathbf{S}_2$, which are defined as follows: $S_0 = \langle D_{2,\,00}\rangle = \langle 1/2(3\cos^2\theta - 1\rangle$, and $S_2 = \langle D_{2,\,02} + D_{2,\,0\text{-}2}\rangle$, where $D_{2,\,00}$, $D_{2,\,02}$, and $D_{2,\,0\text{-}2}$ are the Wigner rotation matrix elements, and θ is the angle between the rotating axis of the nitroxide radical and the director of the bilayer (the preferential orientation of lipid molecules) (17,19). S_0 indicates how strongly the chain segment to which the nitroxide is attached is aligned along the normal to the lipid bilayer. Because a change in S_0 of the headgroup spin label is correlated with hydration/dehydration of the lipid bilayers (20), S_0 is the most important parameter for this study. S_2 is a measure of the molecular nonaxiality of the motion of the spin label. It was found to be much smaller than S_0, with much less sensitivity to changes in bilayer structure induced by TM/lipid interactions. The estimated error from the NLLS fit for the spectra (the standard deviation of converged values of a fitted parameter) is ± 0.01 for S_0 of 5PC and 14PC, and ± 0.006 for S_0 of DPPTC, $\pm 5\%$ for $R_\perp$. In general, the spectra, especially those from chain spin labels, are not very sensitive to $R_\parallel$, so we obtained initial estimates of $N \equiv R_\parallel / R_\perp$ and fixed N in the final fits. This issue arises because $R_\parallel$ is relatively large, and thus its effects on the spectrum are mostly averaged out (21,22). The estimated error is ± 0.05 for the fraction of the spin label in each component spectrum in multiple-component spectral fits.

Turbidity measurements of large unilamellar vesicles of LLE after addition of TM (TM-wt, TM-mut1, and TM-muut2)

For turbidity measurements, 0.6–3.0 μL of 2 mM TM in hexofluoro-isopropanol (HFIP) were added via a Hamilton syringe to 300 μL of LUVs of LLE. The absorbance of the LUV solution (100 μL) at 350 nm was then measured with a Genesys 6 spectrophotometer (Thermo Scientific, Dubai, United Arab Emirates) in a UV-compatible disposable cuvette. Corrections in the absorbance of LUV of LLE were made by subtracting the absorbance of LUV after addition of only HFIP.

RESULTS

The membrane ordering effect of TM-wt is associated with electrostatic interactions of the peptide with negatively charged lipids

As shown in Fig. 1, *A–C* (*solid lines*), when the molar concentration of TM-wt incorporated into MLVs of DMPC/DMPG/Chol = 40/30/30 increases from zero to 1.33×10^{-2} (TM-wt/lipids = 1/75), the S_0 of all three spin labels in the

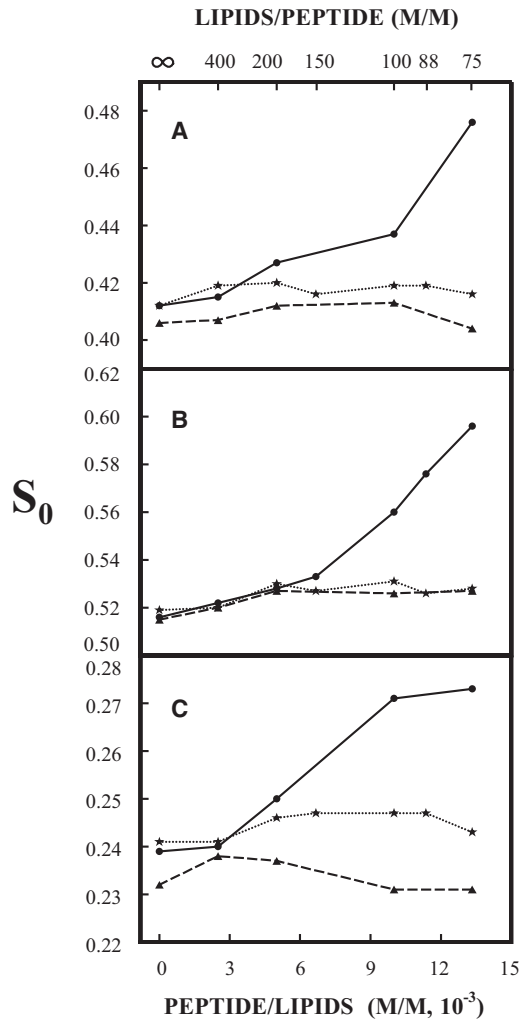

FIGURE 1 Plot of the order parameter S_0 of DPPTC (*A*), 5PC (*B*), and 14PC (*C*) in DMPC/DMPG/Chol = 40/30/30 MLVs versus the concentration of TM-wt (*solid line*) and TM-mut1 (*dotted line*) incorporated in the membranes at 37°C in pH 7 buffer (Tris 10 mM, NaCl 150 mM, EDTA 0.1 mM). The dashed lines in *A–C* are plots of S_0 of the three spin labels in DMPC/DMPG/Chol = 40/30/30 MLVs versus the concentration of TM-wt at 37°C in pH 7 buffer, but the concentration of NaCl is increased to 250 mM.

vesicles at 37°C and pH 7 (10 mM Tris, 150 mM NaCl, 0.1 mM EDTA) increases significantly, i.e., from 0.412 to 0.476 (by 16%) for DPPTC, from 0.52 to 0.60 (by 16%) for 5PC, and from 0.24 to 0.27 (by 14%) for 14PC. The noticeable increases in S_0 start at a concentration of TM-wt around 0.5×10^{-2} (TM-wt/lipids = 1/200). This concentration is the same as that of TM-wt in DMPC/DMPG = 4/1, at which the Fourier transform infrared spectrum of the membrane begins to show a significant change (15).

The NLLS spectral analyses show that all of the spectra of DPPTC and 14PC in the vesicles of DMPC/DMPG/Chol = 40/30/30 can be well fit with a single component. However, the spectra from 5PC show a two-component feature when the concentration of TM-wt in the vesicles is $\geq 1.0 \times 10^{-2}$. (The spectrum with TM-wt/lipids = 1/75 is illustrated in Fig. SF1 of the Supporting Material.) These spectra were successfully simulated with two components with distinct order parameters. The S_0 of the first component (0.55), which is independent of the concentration of TM-wt, is slightly higher than the S_0 of 5PC in vesicles without TM-wt (0.52). The S_0 of the second component is 0.61, 0.64, and 0.69 for the spectra with TM-wt/lipids of 1/100, 1/88, and 1/75, respectively. These values are > 0.59, the order parameter of 5PC at 24.0°C in the gel phase-like domains in pure DMPC bilayers (data not shown). These gel phase-like domains coexist with the liquid crystal phase domains near its main phase transition (23). The second component is less abundant than the first one, with a relative population of 0.21, 0.26, and 0.32, respectively, for the three spectra with the high concentration of TM-wt. Note in Fig. 1 *B* that the values of S_0 of 5PC for the spectra with TM-wt/lipids of 1/100, 1/88, and 1/75 are averaged order parameters over their two components. It is likely that the spectra of DPPTC and 14PC from the vesicles with high concentrations of TM-wt also consist of two components, but they are not resolved. These results indicate that at high concentrations of TM-wt, highly ordered membrane domains are induced in DMPC/DMPG/Chol = 40/30/30 membranes.

The membrane ordering effect by TM-wt depends not only on the concentration of incorporated TM-wt but also the concentration of DMPG in the vesicles. For the case of 5PC, when the concentration of DMPG was reduced from 30 mol % to 10 mol %, giving a mixture of DMPC/DMPG/Chol = 60/10/30, as the concentration of TM-wt was increased from zero to 1.0×10^{-2} (TM-wt/lipids = 1/100), the S_0 of 5PC (at pH 7 and 37°C) increased from 0.51 to 0.57 (*dotted line* in Fig. 2 *A*). However, as the TM-wt/lipids was further increased to 1/88 and 1/75, the S_0 of 5PC decreased to 0.53 and 0.52, respectively. For the case of 14PC, there was almost no change in S_0 (at pH 7 and 37°C) in DMPC/DMPG/Chol = 60/10/30 (*dotted line* in Fig. 2 *B*) as the concentration of TM-wt was increased. When DMPG was completely removed (i.e., in DMPC/Chol = 70/30), the S_0 of 14PC decreased only as TM-wt was incorporated (*dashed line* in Fig. 2 *B*). It can be seen that lowering the concentration of DMPG reduces the membrane ordering effect of TM-wt, and in the vesicles without DMPG incorporation of TM-wt, it only disorders the membrane. (We could not obtain ESR signals from DPPTC in vesicles with a concentration of DMPG < 30% after TM-wt was incorporated; therefore, no results regarding the dependence of S_0 of DPPTC on the concentration of DMPG in these vesicles are presented).

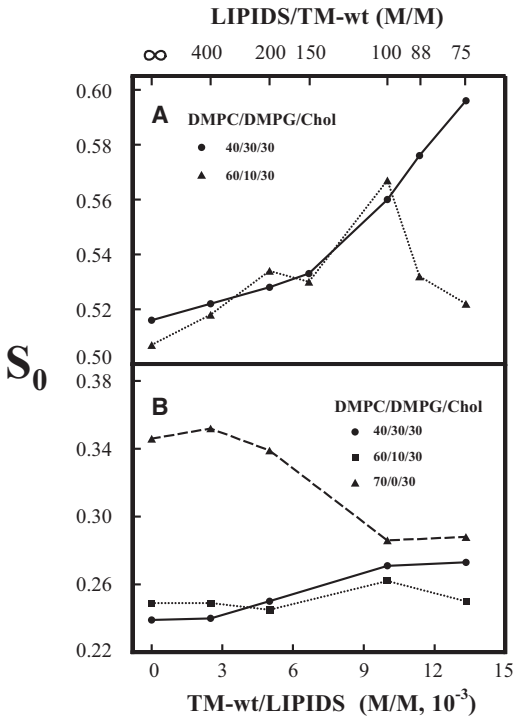

FIGURE 2 (*A*) Plot of the order parameter S_0 of 5PC in DMPC/DMPG/Chol = 40/30/30 (*solid line*) and 60/10/30 (*dotted line*) MLVs versus the concentration of TM-wt incorporated in the membranes at 37°C in pH 7 buffer (Tris 10 mM, NaCl 150 mM, EDTA 0.1 mM). The values of S_0 for lipids/TM-wt = 100, 88, 75 (DMPC/DMPG/Chol = 40/30/30), and for lipids/TM-wt = 100, 88 (DMPC/DMPG/Chol=60/10/30) are averages over two components (see text and Table S1 and Table S4). (*B*) Plot of the order parameter S_0 of 14PC in DMPC/DMPG/Chol = 40/30/30 (*solid line*), 60/10/30 (*dotted line*), and DMPC/Chol=70/30 (*dashed line*) MLVs versus the concentration of TM-wt incorporated in the membranes at 37°C in pH 7 buffer (Tris 10 mM, NaCl 150 mM, EDTA 0.1 mM).

In addition, the membrane ordering effect of TM-wt depends on the ionic strength of the medium. When the concentration of NaCl in the pH 7 buffer was increased from 150 mM to 250 mM, the order parameters of all three spin labels in the vesicles of DMPC/DMPG/Chol = 40/30/30 at 37°C remained constant (within experimental error) as the concentration of TM-wt in the vesicles increased (*dashed lines* in Fig. 1, *A–C*). This is indicative of an ionic interaction of TM-wt with the DMPC/DMPG/Chol = 40/30/30 membranes.

Taken together, the above results suggest that electrostatic interactions between TM-wt and negatively charged DMPG are related to the membrane ordering effect of TM-wt.

The rotational diffusion rates $R_\perp$ and $R_\parallel$, and S_0 of 5PC, 14PC, DPPTC in DMPC/DMPG/Chol = 40/30/30, 60/30/10,

and DMPC/Chol = 70/30 versus the concentration of TM-wt at pH 7 (10 mM Tris, 150 mM NaCl, 0.1 mM EDTA) and 37°C are listed in Table S1, Table S2, Table S3, Table S4, Table S5, and Table S6. It can be seen that upon incorporation of TM-wt, the motion of acyl chains outside the highly ordered membrane domain increases slightly, but increases significantly in the highly ordered membrane domains. TM-wt appears to have the opposite effect on the motion of the headgroups.

Membrane ordering effect of TM-wt for LLE vesicles

We also used the natural lipid mixture LLE, which contains various negatively charged lipids, to test the effect of TM-wt on the membrane ordering. Variations of the S_0 at 37°C and PH7 of the three spin labels in MLVs of LLE with the concentration of TM-wt and with the ionic strength of the buffer are shown in Fig. 3, *A–C* (*solid lines*). When the concentration of TM-wt in LLE increases from zero to 1.33×10^{-2} (TM-wt/lipids = 1/75), the order parameter S_0 of the spin labels increases significantly, i.e., from 0.18 to 0.22 (by 22%) for DPPTC, from 0.43 to 0.48 (by 12%) for 5PC, and from 0.13 to 0.14 (by 8%) for 14PC. It can be seen that the overall membrane ordering effect by TM-wt in LLE is comparable to that in DMPC/DMPG/Chol = 40/30/30. Note that in membranes without TM-wt, the order parameter S_0 of each spin label is lower in LLE (Fig. 3, *A–C*) than in DMPC/DMPG/Chol = 40/30/30 (Fig. 1, *A–C*). This is mainly because LLE contains many lipid species with unsaturated acyl chains.

Similar to the changes in membrane of DMPC/DMPG/Chol = 40/30/30, highly ordered membrane domains are induced by TM-wt in LLE vesicles. All of the spectra of DPPTC and 14PC can be well simulated with a single component, but when the concentration of TM-wt is $\geq 1.0 \times 10^{-2}$, the spectra of 5PC exhibit the same feature as that observed for 5PC spectra in DMPC/DMPG/Chol = 40/30/30. These 5PC spectra need to be fit with two components. The NLLS spectral analysis shows that the S_0 of the more-abundant component (relative population ~75%) is 0.43, which is the same as that in LLE without TM-wt. This value is independent of the concentration of TM-wt in the membrane. The S_0 of the less-abundant component is 0.57, 0.57, and 0.60 for the spectra of 5PC in vesicles with TM-wt/LLE = 1/100, 1/88, and 1/75, respectively.

Again, no membrane ordering effect of TM-wt was observed when the concentration of NaCl in the buffer of LLE vesicles was increased from 150 to 250 mM (*dashed lines* in Fig. 3, *A–C*), indicating that electrostatic interactions between negatively charged lipids and TM-wt are related to the membrane ordering effect in LLE vesicles by TM-wt.

LLE membranes contain not only phosphatidylglycerol (PG) but also significant amounts of other negatively charged lipids, such as phosphatidylinositol (PI) and phosphatidylserine (PS). The concentration of PG in LLE is not available, but it can be roughly estimated as follows: In the total lipid extract of mast cells, the content of PG is 6%, which is less than that of PI (14%) and PS (7%) (24). The amount of PI in LLE is 8% (Avanti, http://www.avantilipids.com). Assuming that the relative amounts of negatively charged lipids in mast cell membrane and in LLE are not significantly different, the content of PG in LLE would likely be <8%. Thus, the comparable membrane ordering effects by TM-wt in LLE and in DMPC/DMPG/Chol = 40/30/30 may imply that in LLE not only the electrostatic interactions of TM-wt with PG but also those with PI and PS contribute to the membrane ordering effect of TM-wt, i.e., the electrostatic interaction between TM-wt and DMPG is not specific.

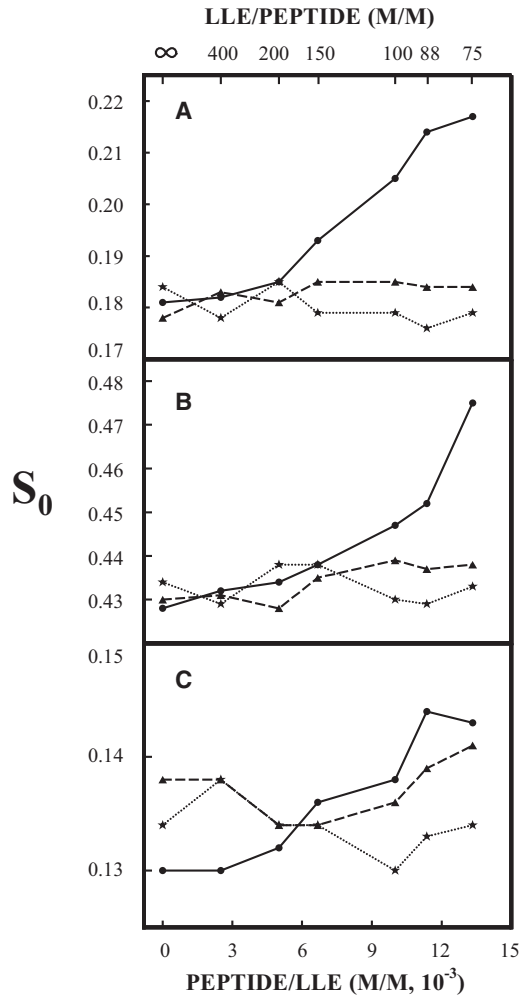

FIGURE 3 Plot of the order parameter S_0 of DPPTC (*A*), 5PC (*B*), and 14PC (*C*) in LLE MLVs versus the concentration of TM-wt (*solid line*) and TM-mut2 (*dotted line*) incorporated in the membranes at 37°C in pH 7 buffer (Tris 10 mM, NaCl 150 mM, EDTA 0.1 mM). The dashed lines in *A–C* are plots of S_0 of the three spin labels in LLE MLVs versus the concentration of TM-wt at 37°C in pH 7 buffer, but the concentration of NaCl is increased to 250 mM.

The rotational diffusion rates $R_\perp$ and $R_\parallel$, and S_0 of 5PC, 14PC, DPPTC in LLE versus the concentration of TM-wt at pH 7 (10 mM Tris, 150 mM NaCl, 0.1 mM EDTA) and 37°C are listed in Table S7, Table S8, and Table S9. It can be seen that the effects of TM-wt incorporation on the motion of LLE membranes are similar to those observed for the DMPC/DMPG/Chol membranes.

Substitution of the lysine residue in TM-wt with a glutamic acid residue abolishes the membrane ordering effect

According to Tatulian and Tamm (15), the helical coiled coils of TM-wt in DMPC/DMPG bilayers are aligned perpendicular to the plane of the bilayer. This alignment allows two positively charged amino acid residues, the lysine near the N-terminus and the arginine near the C-terminus (both located at the interface of the bilayer), to interact with the negatively charged headgroups in the vesicles. We are more interested in the interactions of lipids with the lysine than with the arginine, for two reasons. First, the N-terminus lysine residue of TM in HA is positioned near the surface of the outer leaflet of the viral membrane, whereas the C-terminus arginine residue is positioned near the surface of the inner leaflet of the viral membrane. Thus, the former can have a more direct effect on interactions between the viral and target membranes during viral fusion than the latter. Second, lysine is a highly conserved residue in amino acid sequences of the TM in HA of influenza, but the arginine is not (15). We substituted the lysine with a negatively charged residue glutamic acid and incorporated the mutated peptide (TM-mut1) into MLVs of DMPC/DMPG/Chol = 40/30/30. We found that at pH 7 and 37°C, the S_0 of all three spin labels in the vesicles hardly changed with the concentration of TM-mut1 in the vesicles (*dotted lines* in Fig. 1, *A–C*). Thus, the N-terminus lysine is important for the membrane ordering effect by TM-wt.

Mutation of the conserved residue leucine also abolishes the membrane ordering effect

In addition to the lysine, the leucine residue in TM-wt near the N-terminus is also a highly conserved residue in influenza HA. To test whether it is also related to the increased ordering of membranes by TM-wt, we mutated the leucine with a hydrophobic residue alanine. We found that incorporation of the mutated peptide (TM-mut2) into MLVs of LLE had no effect on the ordering of the three spin labels in the vesicles (*dotted lines* in Fig. 3, *A–C*), indicating that the leucine residue near the N-terminus is also important for the membrane ordering effect of TM-wt. This implies that the hydrophobic interaction between TM-wt and the membrane also plays a role in the enhanced membrane ordering. However, the contributions of the electrostatic interaction and the hydrophobic interaction between TM-wt and the lipid bilayers to the membrane ordering effect are not simply additive. It is possible that a mutation of leucine could modify the conformation of the helical coiled coil of TM-wt, making the lysine residue in TM-mut2 inaccessible to the negatively charged headgroups.

The rotational diffusion rates $R_\perp$ and $R_\parallel$, and S_0 of 5PC, 14PC, DPPTC in DMPC/DMPG/Chol = 40/30/30 versus the concentration of TM-mut1, and in LLE versus the concentration of TM-mut2 at pH 7 (10 mM Tris, 150 mM NaCl, 0.1 mM EDTA) and 37°C are listed in Table S10, Table S11, Table S12, Table S13, Table S14, and Table S15. It can be seen that incorporation of both mutants had no effect on the motion and ordering of the membranes.

An increase in the turbidity of LUVs of LLE induced by TM-wt is correlated with the membrane ordering effect of TM-wt

In Fig. 4, the absorbance of the LUVs of LLE at 350 nm is plotted versus the concentrations of TM-wt, TM-mut1, and TM-mut2 added to the vesicle solution. It can be seen that the turbidity of the LUVs increased significantly only after addition of TM-wt, and no change in the turbidity of the LUVs was observed after addition of the two mutants. These results are correlated with significant increases in the membrane ordering of DMPC/DMPG/Chol (40/30/30) and LLE vesicles incorporated with TM-wt, but no change in the membrane ordering of DMPC/DMPG/Chol (40/30/30) and LLE vesicles incorporated with the two mutants. As shown in Fig. 4, the molar ratio TM-wt/LLE for a noticeable increase in turbidity, 1/190, is nearly the same as 1/200, the molar ratio TM-wt/LLE for a noticeable increase in the order parameters S_0 of the spin labels in those vesicles, as shown in Figs. 1, *A–C*, and 3, *A–C*. An increase in the turbidity of the LUV solutions is an indication of aggregation of the vesicles (25). Aggregation of LLE vesicles by

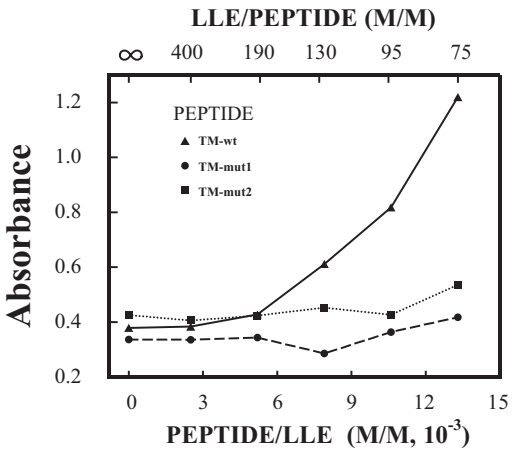

FIGURE 4 Plot of absorbance of LUV of LLE at 350 nm versus the amount of peptide TM-wt (*solid line*), TM-mut1 (*dashed line*), and TM-mut2 (*dotted line*) added to the LUV.

TM-wt was verified by transmission electron microscopy (data not shown). Because an increase in membrane surface ordering reflects membrane dehydration (20,26,27), this reveals that aggregation of the LLE vesicles is associated with membrane dehydration by TM-wt.

DISCUSSION

The main effect of TM-wt on the membrane structure in DMPC/DMPG/Chol = 40/30/30 and LLE vesicles that we found is that TM-wt induces highly ordered membrane domains in the vesicles, and this correlates with LLE vesicle aggregation. Below, we discuss the implications of increased ordering of membrane domains for vesicle aggregation and viral membrane fusion.

Highly ordered membrane domains are discrete

Previous studies reported membrane domain formation (or phase separation) in phosphatidylcholine (PC) and PG mixtures induced by a peptide containing six positively charged residues (28), and in phosphatidic acid, PG, PS, and PC mixtures induced by human myelin basic protein (29). In both cases, it was suggested that the phase separation was driven by electrostatic interactions between negatively charged lipids and the positively charged peptide/protein. In addition, it was recently shown that electrostatic interactions are also involved in the formation of a pinched multilamellar structure of aggregates of a highly basic protein, lysozyme, in PS-containing membranes (30). Thus, we suggest that the highly ordered membrane domains in DMPC/DMPG/Chol = 40/30/30 and LLE vesicles are associated with the electrostatic interactions between the inserted TM-wt and negatively charged lipids, which are enriched in the domains.

As shown above, the fraction of 5PC in the highly ordered membrane domain of DMPC/DMPG/Chol = 40/30/30 and LLE vesicles is 20–30%. For 5PC, a spin-labeled PC, the interaction of its zwitterionic headgroup with TM-wt is weaker than the electrostatic interactions of the negatively charged headgroups with TM-wt. Thus, 5PC would be less favorably partitioned into the highly ordered membrane domains. That is, the actual amount of lipids contained in the highly ordered membrane domains may be more than 20–30% of that in the whole membrane, but it is not likely to be > 50% of the total lipids. This means that these membrane domains may exist as discrete regions dispersed in the vesicle membranes. Because the ordering of the membrane outside these highly ordered membrane domains is the same as or only slightly higher than the ordering of the membrane without TM-wt in LLE and DMPC/DMPG/Chol = 40/30/30 vesicles, the membrane ordering effect of TM-wt is localized in these discrete domains. Given the correlation of increased membrane ordering with membrane dehydration, we also suggest that these domains are highly dehydrated (20,26,27).

Hypothesis for the formation of a highly ordered water capillary bridge between two highly ordered membrane domains

Previous studies on PS vesicle aggregation and fusion induced by Ca^{2+} and Mg^{2+} (13,14,31) suggested that membrane dehydration (i.e., membrane surface hydrophobicity) is important for vesicle aggregation and membrane fusion. On the basis of the observed correlation between membrane ordering (dehydration) and LLE vesicle aggregation, we propose the following mechanism for TM-induced vesicle aggregation: 1) To reduce exposure of the hydrophobic domain surfaces to the aqueous solution, aggregation of LLE vesicles would most likely occur between these membrane domains. 2) Two aggregated LLE vesicles are connected by a water capillary bridge between two highly ordered membrane domains, as illustrated in Fig. 5. A capillary bridge of a liquid (water or a solvent) will form when two surfaces (plane or curved surface), which are wetted by the liquid, are brought close together (the liquid-air interface is a meniscus, hence the capillary bridge (32,33)). 3) Because of the correlation between the ordering of the headgroups and the ordering of the membrane surface water (27), the water on the surface of the highly ordered membrane domains is also highly ordered. Thus, the water capillary bridge between two highly ordered membrane domains (*green* in Fig. 5) is made up of the highly ordered water on the membrane domain surface that is interfaced with the surrounding nonordered bulk water (*blue* in Fig. 5). The orientations of the water molecules and hydrogen-bonding structure in the two water phases are significantly different (27).

Suppose the interfacial tension between the two water phases is γ. According to the Young-Laplace equation, $\Delta p = 2\gamma/R$, which relates the pressure differences across

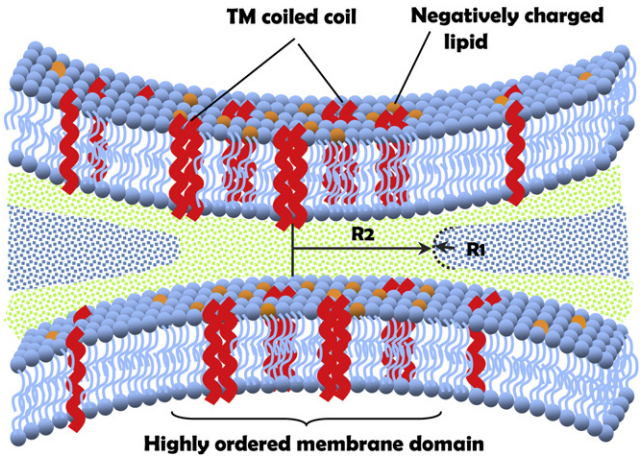

FIGURE 5 Suggested mechanism for aggregation of vesicles containing negatively charged lipids induced by TM-wt. Two highly ordered membrane domains enriched in TM-wt and negatively charged lipids are connected by a highly ordered water capillary bridge (*green*). The water bridge is interfaced with the nonordered bulk water (*blue*). The principal radii of curvature of the interface are R_1 and R_2, respectively.

the interface, Δp, with γ and R (the principal radius of the interface meniscus), the pressure inside the bridge is anisotropic. That is, the pressure along the direction of the symmetry axis of the bridge is negative due to the negative principal curvature $1/R_1$, whereas the pressure in all directions perpendicular to the axis is positive due to the positive principal curvature $1/R_2$. This surface tension effect, a boundary condition for the mechanical equilibrium of the water capillary bridge, is consistent with the Maxwell stress tensor inside the bridge, which has a negative z-component (a stretching force along the symmetry axis of the bridge), and positive x- and y-components (compressing forces). This stress tensor is generated by an electric field inside the bridge as a result of polarization of water molecules, i.e., due to the preferential orientation of electric dipoles of water molecule along the axis of the bridge (27). The capillary negative pressure in water capillary bridge 108 nm high observed in silicon-based nanochannels was previously estimated to be $\sim -17 \pm 10$ bar (34). The attractive forces in the water bridge between two LLE vesicles would probably be much larger than this value because the distance between the two aggregated LLE vesicles is <10 nm, as revealed in our transmission electron micrographs (data not shown).

The main points of the suggested mechanism of TM-induced LLE vesicle aggregation can be summarized as follows: Vesicle aggregation is mediated by membrane surface water and headgroups through the formation of a highly ordered water capillary bridge between two highly ordered membrane domains. If somehow the membrane domain is more ordered (i.e., more dehydrated), the water in the bridge will also be more ordered. Thus, the attractive forces between the membrane domains generated by stronger polarization of the water would be larger, leading to more significant vesicle aggregation.

Implications for viral membrane fusion

In a recent study (35), electron cryotomography images of fusion between influenza virus particles and PC vesicles showed that after acidification, a vesicle was caught by a virus particle and dragged toward it, so that the vesicle became funnel-shaped and breached in the mouth of the funnel at the contact zone between the vesicle and the virus particle. Conceivably, a very strong attractive force that is highly localized in the apposed membrane region between the vesicle and the virus particle is responsible for such a dramatic vesicle membrane deformation. This raises the question as to how this force is generated.

It is commonly accepted that after low-pH triggering occurs, HA-mediated viral fusion goes through conformational changes of HA trimers from a prehairpin that is an extended structure of the HA trimer to a complete hairpin that corresponds to a state of complete fusion. In the prehairpin state, the FP is inserted into the cellular membrane and the TM domain is anchored in the viral membrane, such that two membranes are connected (1–3). Insertion of FP dehydrates the cellular membrane around the FP (10). On the other hand, it is likely that the highly ordered membrane domains induced by TM-wt that we observed in membranes containing negatively charged lipids may also exist in the viral membrane, so that the viral membrane around the HA trimers would be dehydrated. Now we would like to extend our suggested mechanism for vesicle aggregation to viral fusion. We suggest that in the prehairpin state, a highly ordered water capillary bridge may form between the dehydrated cellular and viral membranes around the HA hairpins. The attractive forces in the water capillary bridge, which pull the two membranes together, facilitate the conformational change of HA trimers from a prehairpin to a complete hairpin. These forces would be the same as those observed in the initial stage of fusion between PC vesicles and influenza virus particles mentioned above (35). They are hydrophobic forces between the locally dehydrated membranes due to changes in the structure of membrane surface water and headgroups induced by HA-lipid interactions. They are not likely generated only as a result of conformational changes of HA, as suggested by a spring-loaded mechanism (36).

We believe we are beginning to understand why membrane dehydration is crucial for viral fusion. Thus, we also suggest that in addition to the fusion peptide and the TM domain, a kinked loop region in HA2, which has been shown to be self-clustered and able to induce vesicle aggregation at fusion-active pH (37–39), may also dehydrate the cellular membrane, making the fusion site more hydrophobic and thus promoting HA-mediated viral fusion.

The above discussion implies that fusion proteins interact with both viral and cellular membranes, modifying the structures of the membranes, and the ensured evolution of membrane fusion is regulated by the existing physicochemical principles for membrane remodeling. Thus, both fusion proteins and membranes play an active role in viral fusion.

CONCLUSIONS

Two conserved residues, the N-terminus lysine and leucine, are important for the membrane ordering effect by TM-wt. This effect is highlighted by the formation of highly ordered membrane domains that is driven by electrostatic interactions between the positively charged TM-wt and negatively charged lipids. The correlation between the membrane ordering effect and aggregation of LLE vesicles suggests that the hydrophobic interaction between the highly ordered membrane domains is important for vesicle aggregation.

SUPPORTING MATERIAL

Sixteen tables and one figure are available at http://www.biophysj.org/biophysj/supplemental/S0006-3495(10)01383-4.

This work was supported by grants from the National Institutes of Health/National Institute of Biomedical Imaging and Bioengineering R01EB003150 and National Institutes of Health/National Center for Research Resources P41RR016292).

REFERENCES

1. White, J. M., S. E. Delos, …, K. Schornberg. 2008. Structures and mechanisms of viral membrane fusion proteins: multiple variations on a common theme. *Crit. Rev. Biochem. Mol. Biol.* 43:189–219.
2. Martens, S., and H. T. McMahon. 2008. Mechanisms of membrane fusion: disparate players and common principles. *Nat. Rev. Mol. Cell Biol.* 9:543–556.
3. Harrison, S. C. 2008. Viral membrane fusion. *Nat. Struct. Mol. Biol.* 15:690–698.
4. Peisajovich, S. G., and Y. Shai. 2003. Viral fusion proteins: multiple regions contribute to membrane fusion. *Biochim. Biophys. Acta.* 1614:122–129.
5. Li, Z., and G. W. Blissard. 2008. Functional analysis of the transmembrane (TM) domain of the *Autographa californica* multicapsid nucleopolyhedrovirus GP64 protein: substitution of heterologous TM domains. *J. Virol.* 82:3329–3341.
6. Li, Z., and G. W. Blissard. 2009. The *Autographa californica* multicapsid nucleopolyhedrovirus GP64 protein: analysis of transmembrane domain length and sequence requirements. *J. Virol.* 83:4447–4461.
7. Broer, R., B. Boson, …, J. Corver. 2006. Important role for the transmembrane domain of severe acute respiratory syndrome coronavirus spike protein during entry. *J. Virol.* 80:1302–1310.
8. Kemble, G. W., T. Danieli, and J. M. White. 1994. Lipid-anchored influenza hemagglutinin promotes hemifusion, not complete fusion. *Cell.* 76:383–391.
9. Takeda, M., G. P. Leser, C. J. Russell, and R. A. Lamb. 2003. Influenza virus hemagglutinin concentrates in lipid raft microdomains for efficient viral fusion. *Proc. Natl. Acad. Sci. USA.* 100:14610–14617.
10. Ge, M., and J. H. Freed. 2009. Fusion peptide from influenza hemagglutinin increases membrane surface order: an electron-spin resonance study. *Biophys. J.* 96:4925–4934.
11. Hoekstra, D. 1982. Role of lipid phase separations and membrane hydration in phospholipid vesicle fusion. *Biochemistry.* 21:2833–2840.
12. Han, X., D. A. Steinhauer, …, L. K. Tamm. 1999. Interaction of mutant influenza virus hemagglutinin fusion peptides with lipid bilayers: probing the role of hydrophobic residue size in the central region of the fusion peptide. *Biochemistry.* 38:15052–15059.
13. Arnold, K. 1995. Cation-induced vesicle fusion modulated by polymers and proteins. *In* Structure and Dynamics of Membranes. R. Lipowsky and E. Sackman, editors. Elsevier Science, Amsterdam/New York. 903–957.
14. Wilschut, J., N. Düzgüneş, and D. Papahadjopoulos. 1981. Calcium/magnesium specificity in membrane fusion: kinetics of aggregation and fusion of phosphatidylserine vesicles and the role of bilayer curvature. *Biochemistry.* 20:3126–3133.
15. Tatulian, S. A., and L. K. Tamm. 2000. Secondary structure, orientation, oligomerization, and lipid interactions of the transmembrane domain of influenza hemagglutinin. *Biochemistry.* 39:496–507.
16. Chang, D.-K., S.-F. Cheng, …, Y. T. Liu. 2008. Membrane interaction and structure of the transmembrane domain of influenza hemagglutinin and its fusion peptide complex. *BMC Biol.* 6:2.
17. Budil, D. E., S. Lee, …, J. H. Freed. 1996. Nonlinear-least-squares analysis of slow-motion EPR spectra in one and two dimensions using a modified Levenberg-Marquardt algorithm. *J. Magn. Reson. A.* 120: 155–189.
18. Meirovitch, E., D. Igner, …, J. H. Freed. 1982. Electron-spin relaxation and ordering in smectic and supercooled nematic liquid crystals. *J. Chem. Phys.* 77:3915–3938.
19. Schneider, D. J., and J. H. And. Freed. 1989. Calculating slow motional magnetic resonance spectra: a user's guide. *In* Spin Labeling Theory and Applications, Vol. *8*. L. J. Berliner and J. Reuben, editors. Plenum Press, New York. 1–76.
20. Ge, M., and J. H. Freed. 2003. Hydration, structure, and molecular interactions in the headgroup region of dioleoylphospatidylcholine bilayers: an electron-spin resonance study. *Biophys. J.* 85:4023–4040.
21. Ge, M., and J. H. Freed. 1999. Electron-spin resonance study of aggregation of gramicidin in dipalmitoylphosphatidylcholine bilayers and hydrophobic mismatch. *Biophys. J.* 76:264–280.
22. Ge, M., A. Gidwani, …, J. H. Freed. 2003. Ordered and disordered phases coexist in plasma membrane vesicles of RBL-2H3 mast cells. An ESR study. *Biophys. J.* 85:1278–1288.
23. Wittebort, R. J., C. F. Schmidt, and R. G. Griffin. 1981. Solid-state carbon-13 nuclear magnetic resonance of the lecithin gel to liquid-crystalline phase transition. *Biochemistry.* 20:4223–4228.
24. Fridriksson, E. K., P. A. Shipkova, …, F. W. McLafferty. 1999. Quantitative analysis of phospholipids in functionally important membrane domains from RBL-2H3 mast cells using tandem high-resolution mass spectrometry. *Biochemistry.* 38:8056–8063.
25. Ohki, S., N. Düzgüneş, and K. Leonards. 1982. Phospholipid vesicle aggregation: effect of monovalent and divalent ions. *Biochemistry.* 21:2127–2133.
26. Arnold, K., A. Hermman, …, L. Pratsch. 1987. Water-mediated effect of PEG on membrane properties and fusion. *In* Molecular Mechanism of Membrane Fusion. S. Ohki, D. Doyle, T. D. Flanagan, S. W. Hui, and E. Mayhew., editors. Plenum Press, New York/London. 255–273.
27. Binder, H. 2007. Water near lipid membranes as seen by infrared spectroscopy. *Eur. Biophys. J.* 36:265–279.
28. Gawrisch, K., J. A. Barry, …, J. A. Ferretti. 1995. Role of interactions at the lipid-water interface for domain formation. *Mol. Membr. Biol.* 12:83–88.
29. Boggs, J. M., M. A. Moscarello, and D. Papahadjopoulos. 1977. Phase separation of acidic and neutral phospholipids induced by human myelin basic protein. *Biochemistry.* 16:5420–5426.
30. Coutinho, A., L. M. S. Loura, …, M. Prieto. 2008. Pinched multilamellar structure of aggregates of lysozyme and phosphatidylserine-containing membranes revealed by FRET. *Biophys. J.* 95:4726–4736.
31. Ohki, S. 1987. Surface tension, hydration energy and membrane fusion. *In* Molecular Mechanism of Membrane Fusion. S. Ohki, D. Doyle, T. D. Flanagan, S. W. Hui, and E. Mayhew, editors. Plenum Press, New York/London. 123–138.
32. Fisher, L. R., and J. N. Israelachvili. 1979. Direct experimental verification of the Kelvin equation for capillary condensation. *Nature.* 277:548–549.
33. van Honschoten, J. W., N. Brunets, and N. R. Tas. 2010. Capillarity at the nanoscale. *Chem. Soc. Rev.* 39:1096–1114.
34. Tas, N. R., P. Mela, …, A. van den Berg. 2003. Capillary induced negative pressure of water plugs in nanochannels. *Nano Lett.* 3:1537–1540.
35. Lee, K. K. 2010. Architecture of a nascent viral fusion pore. *EMBO J.* 29:1299–1311.
36. Carr, C. M., and P. S. Kim. 1993. A spring-loaded mechanism for the conformational change of influenza hemagglutinin. *Cell.* 73:823–832.
37. Epand, R. F., J. C. Macosko, …, R. M. Epand. 1999. The ectodomain of HA2 of influenza virus promotes rapid pH dependent membrane fusion. *J. Mol. Biol.* 286:489–503.
38. Kim, C.-H., J. C. Macosko, and Y.-K. Shin. 1998. The mechanism for low-pH-induced clustering of phospholipid vesicles carrying the HA2 ectodomain of influenza hemagglutinin. *Biochemistry.* 37:137–144.
39. LeDuc, D. L., Y.-K. Shin, …, R. M. Epand. 2000. Factors determining vesicular lipid mixing induced by shortened constructs of influenza hemagglutinin. *Biochemistry.* 39:2733–2739.